

UDC 544.431.8+544.015.4

**SIZE AND SHAPE EFFECT ON THE PHASE TRANSITIONS IN A SMALL SYSTEM WITH FRACTAL INTERPHASE BOUNDARIES**Fedoseev V. B.<sup>1</sup>, Potapov A.A.<sup>2</sup>, Shishulin A.V.<sup>3</sup>, Fedoseeva E.N.<sup>3</sup><sup>1</sup>Razuvaev Institute of Organometallic Chemistry RAS, Nizhny Novgorod, Russia, [vbfedoseev@yandex.ru](mailto:vbfedoseev@yandex.ru)<sup>2</sup>V.A. Kotelnikov Institute of Radio Engineering and Electronics of RAS, Moscow, Russia, [potapov@cplire.ru](mailto:potapov@cplire.ru)<sup>3</sup>N.I. Lobachevsky Nizhny Novgorod State University, Nizhny Novgorod, Russia [Chichouline\\_Alex@live.ru](mailto:Chichouline_Alex@live.ru)

*Shape effect as a property of small volume systems is considered in an example of a stratifying solid solution. Phase diagrams, which demonstrate phase equilibria dependence on the shape of system's boundaries, are calculated by the methods of equilibrium chemical thermodynamics. Shape of system is modeled by coefficient  $k_f$ , which is equal to the ratio between the system's area and the area of a sphere of the same volume. Core-shell configurations are considered, where system's external boundary shape is a parameter and can differ and core-phase's form is spherical. Shell-phases external boundary form affects components' mutual solubility, upper critical temperature of stratification and core- and shell-phases volume ratio. The area of heterogeneous states' thermodynamical stability decreases and the area of metastable states' increases with the growth of  $k_f$ . This model can also be used when shell-phase's shape is fractal. In this case, on the one hand, the fractal dimension can be regarded as a thermodynamical function, on the other hand, it can be measured experimentally.*

**Keywords:** phase transitions, size effects, shape effect, core-shell, fractal surface

**Introduction**

The construction of phase diagrams for small volume systems has become one of the new trends in chemical thermodynamics. The need to recalculate the diagrams is due to the fact that the displacement of characteristic lines and points in phase diagrams for nanoscale systems can exceed hundreds of degrees [1]. The system volume reduction can be accompanied by the splitting of the phase diagram and the appearance of unusual metastable phases [2-6]. The calculation of phase equilibria in small volume systems is based on minimization of Gibbs energy taking into account the energy of interphase boundaries [7-9]. The contribution of surface energy becomes significant when the system or individual phases have submicron sizes. The size effect affects the phase equilibrium, changing the composition and volume of coexisting phases, changing the thermodynamic stability of metastable phases [10]. In this paper, a thermodynamic approach to simulate systems with various morphologies is used.

In a closed small-volume system, the area of the interphase boundaries and their energies depend substantially on the shape of the system and the interphase boundaries; and therefore the estimate of the phase composition in small volume systems without specifying geometric characteristics is incorrect. Most estimates are performed for the simplest configurations with a spherical symmetry of the core-shell type [9,11] or "janus" [3, 11] or an axial symmetry with a plane [12,13] interphase boundary. These configurations are convenient for simulation. However, real systems have more complex structures. An example is the transformation of micron-sized hydrocarbon droplets dispersed in surfactant solutions [14], upon cooling of which many different configurations are observed.

In this paper, a system with a core-shell configuration, which often occurs at homogeneous nucleation of phases, is considered. In contrast to the estimates [6, 10], let us assume that the shape of the outer surface of the shell-phase is one of the parameters of the model. It is determined by

external boundaries, for example, the walls of a solid matrix or the boundaries of neighboring grains and can vary with deformation of the material.

## 1. Theoretical part

To demonstrate the effect, let us use the Bi-Sb alloy described in [6]. Consider a closed system with a core-shell configuration of  $x = 0.5$  equimolar composition, where  $x$  is a mole fraction of Sb. The core-phase does not touch boundaries. The Bi-Sb alloy is stratified into two solid solutions [15]. For a closed system of equimolar composition, the conservation conditions have the form

$$n_1 = n_2 = 0.5n, \quad V = 0.5n(V_1 + V_2), \quad n_{ic} = \theta_i n_i, \quad n_{is} = (1 - \theta_i)n_i, \quad i = 1, 2, \quad (1)$$

where  $n$  is the total number of moles in the system;  $n_{if}$  is the number of moles of  $i$  component in  $f = c, s$  phase;  $V$  is the volume of the system;  $V_i$  are the molar volumes of the components; the indices 1 and 2 correspond to Sb and Bi;  $c$  and  $s$  indices stand for the core- and shell-phases respectively.  $\theta_i = \frac{n_{ic}}{n_{ic} + n_{is}}$  values correspond to the fractions of the components in the core-phase composition. Since  $0 \leq \theta_i \leq 1$ , it is convenient to use them when changing variables and analyzing simulation results. Concentrations (molar fractions) of the components in phases

$$x_{1f} = \frac{n_{1f}}{n_{1f} + n_{2f}}, \quad x_{2f} = 1 - x_{1f}, \quad f = c, s. \quad (2)$$

Equations (1)-(2) completely govern the quantitative composition of the system, individual phases and the phase volumes

$$V_f = n_{1f}V_1 + n_{2f}V_2, \quad f = c, s. \quad (3)$$

The area of interphase boundaries depends on the shape of the system and the core-phase. By hypothesis, the core-phase has a spherical shape, so  $A_c$  interphase boundary area and its  $R_c$  radius are determined by the volume of  $V_c$  core-phase or by the amounts of a substance that have passed to the core-phase (3)

$$R_c = \left( \frac{3}{4\pi} V_c \right)^{\frac{1}{3}}, \quad A_c = 4\pi R_c^2. \quad (4)$$

Such a simplification is incorrect if the spherical core-phase falls outside the limits of the system. The equilibrium composition of the phases corresponds to the constrained minimum of Gibbs function

$$g = (n_{1c} + n_{2c})G(x_{1c}, T) + (n_{1s} + n_{2s})G(x_{1s}, T) + g_{surf}, \quad (5)$$

where  $G(x, T)$  is the molar Gibbs function of Bi-Sb solid solution [15]. The contribution of the interphase surfaces to Gibbs energy has the form

$$g_{surf} = \sigma_s A_s + \sigma_{cs} A_c, \quad (6)$$

where  $\sigma_s$  is the surface energy of the solid solution at the outer boundary;  $\sigma_{cs}$  is the energy of the interface between the core- and shell-phases;  $A_c$  and  $A_s$  are the surface areas of the core- and shell-phases. The surface energy of the pure components is taken from [16]. For the interphase boundary the following approximation is used:

$$\sigma_{cs} = 0.5(\sigma(x_c) + \sigma(x_s)). \tag{7}$$

The total contribution of the surface energy

$$g_{surf} = (x_s \sigma_{Sb} + (1 - x_s) \sigma_{Bi}) A_s + 0.5(x_s \sigma_{Sb} + (1 - x_s) \sigma_{Bi} + x_c \sigma_{Sb} + (1 - x_c) \sigma_{Bi}) A_c.$$

Recalculation of the Gibbs function (5) per a mole of the mixture

$$G = \frac{g}{n_1 + n_2} \tag{8}$$

makes it possible to compare systems of different size, shape and composition.

As an example, a calculation for a system which volume is equivalent to the volume of a sphere of  $R_0 = 200$  nm radius is given. The Gibbs function (8) in  $(\theta_1, \theta_2)$  coordinates is shown in Fig. 1a.  $G(0,0) = 0$  homogeneous state is accepted as a zero level.

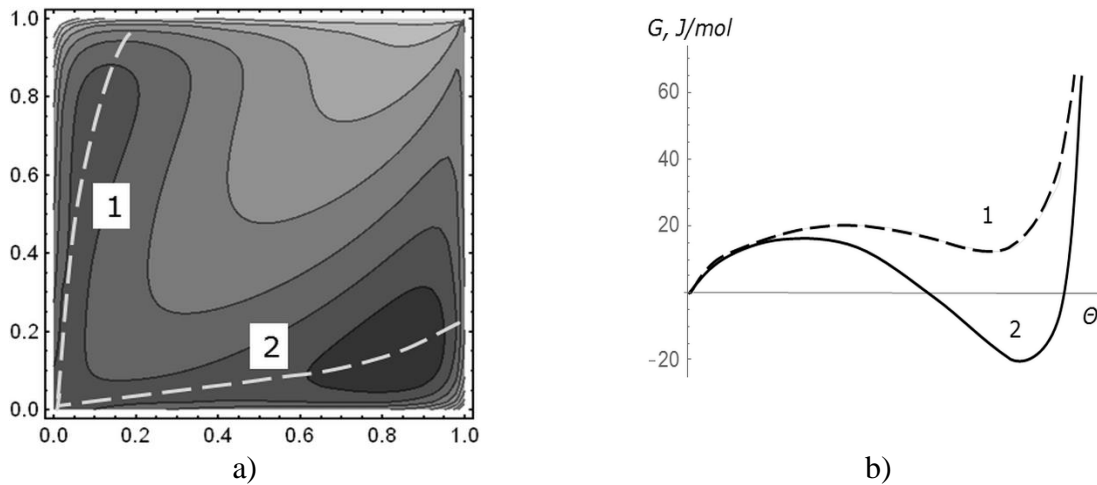


**Fig.1.** The darker shade corresponds to minimums. The dashed lines are the trajectories passing through 1) the local minimum, 2) the global minimum and the homogeneous state (0,0):

a) the projection of the Gibbs function in  $(\theta_1, \theta_2)$  coordinates for a spherical core-shell particle of  $R_0 = 200$  nm radius at  $T = 280$  K; b) the change in the Gibbs function along trajectories 1 and 2.

The system (Fig. 1) has three stable states. The global minimum corresponds to the heterogeneous state when Sb predominates in the core-phase. As related to it, the homogeneous state and the second heterogeneous state, when Bi predominates in the core-phase, are metastable.

## 2. Results and Discussion

### 2.1 The shape effect

Let us consider the shape effect by changing the shape of the same system (Bi-Sb mixture at  $x = 0.5$ ) having a volume equal to the volume of a sphere of  $R_0 = 100$  nm radius. The spherical configuration has a minimal boundary area, so any deformation of the system is accompanied by an increase in the surface area. On that basis, let us introduce  $k_f = \frac{S}{S_0}$  shape coefficient in the form of the ratio of the surface area of the considered figure  $S$  and the sphere of the same volume  $S_0$ . In this case, the change in shape reduces to adding  $k_f$  factor to equation (6) or

$$A_s = k_f A_{s,0}, \quad \text{where} \quad A_{s,0} = 4\pi R_0^2.$$

Fig. 2 shows an example demonstrating how a change in shape affects the phase diagram. All diagrams show the solid solution breakdown curve for a macroscopic system (the separation arc).

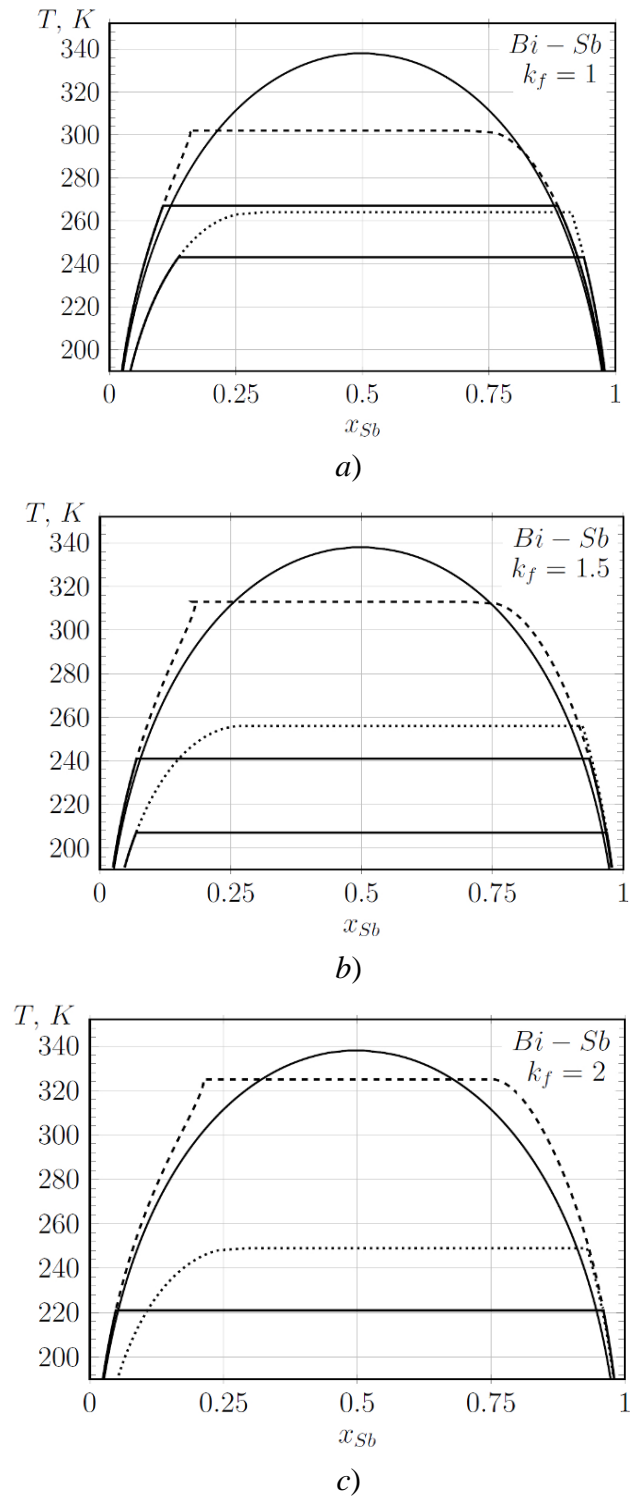


**Fig. 2.** The solubility diagram of the Bi-Sb alloy for a particle with  $R_0 = 100$  nm having a core-shell configuration at : a)  $k_f = 1$ ; b)  $k_f = 1.5$ ; c)  $k_f = 2$ .

Curves of a trapezoidal shape correspond to binodals for a small volume system. Solid lines limit the region in which a heterogeneous state is more favourable than a homogeneous one  $G(\theta_1, \theta_2) < G(0, 0)$ .

The dashed and dotted lines that continue them, bound the region in which the heterogeneous state is metastable with respect to the homogeneous one  $G(\theta_1, \theta_2) > G(0, 0)$ . The change in shape is accompanied by a significant change in the upper critical dissolution temperature (UCDT) and the composition of the coexisting phases. Moreover, with increasing  $k_f$ , the temperature range within which the heterogeneous state is metastable, grows. In this region, the system can either form a continuous series of solid solutions, or be in a heterogeneous state.

Care should be taken when considering configurations with large  $k_f$  values. The radius of the core-phase should not exceed the radius of the sphere inscribed in the system (for example, the length of the minor semiaxis for the spheroid). High  $k_f$  values can be realized if the shell-phase has the form of a fractal coating over the core-phase. In this case

$$A_s = CV^{2/D}, \quad k_f = \frac{C}{4\pi} \frac{V^{2/D}}{\left(\frac{3V}{4\pi}\right)^{2/3}} \sim \tilde{C}V^{2\left(\frac{3-D}{3D}\right)}, \quad \tilde{C} \geq 1,$$

where  $D$  is the fractal dimension of the system surface,  $C$  is the numerical coefficient.

## 2.2 The model with a fractal surface

The model with a fractal surface reproduces all the regularities described above for a fixed volume. However, for a fractal shell-phase,  $k_f$  value depends on the system volume if  $D = \text{const}$ , or, at  $k_f = \text{const}$ , it is the fractal dimension that will depend on the volume. Apparently, a change in the volume of the system will be accompanied by a simultaneous change in  $D$  and  $k_f$ ; and the value of  $D$  can be regarded as one of thermodynamic functions [17, 18].

Equally interesting is the case when a core-phase formed inside the spherical drop has a fractal dimension. This situation is often realized during formation of polycrystals or suspensions when the droplets dry up. Observations show that some substances (for example, many alkali metal salts) in a small volume often form single crystals, while the formation of polydisperse deposits is characteristic for the majority of organic substances and crystalline hydrates of inorganic salts. Examples that demonstrate this effect are shown in Figure 3.

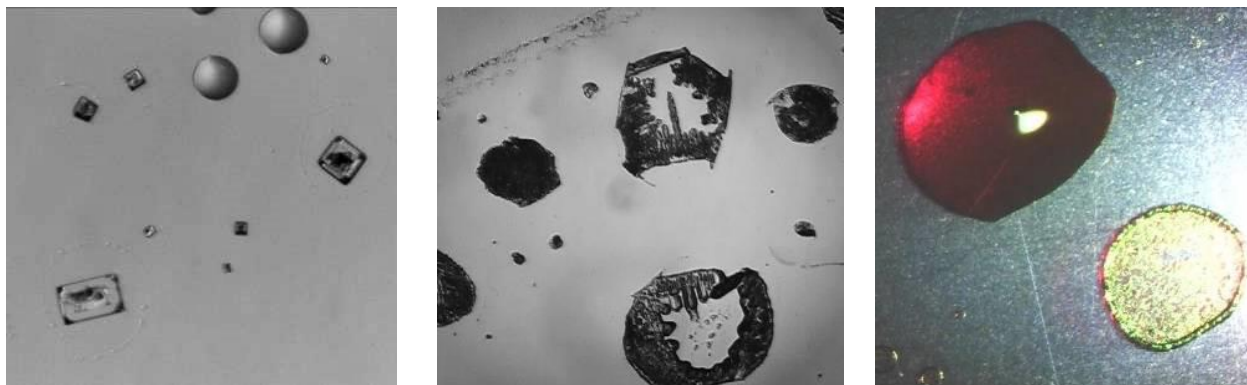


**Fig. 3.** The structures formed when drops of aqueous solutions dry up: KCl – on the left; hydroquinone – in the center on the glass substrate; rhodamine B on the lavsan - on the right ( $200 \times 200 \mu\text{m}$ ).

For this case, the fractal dimension is taken into account by adding  $k_f$  coefficient in calculating the surface area of the core-phase in (6)

$$A_c = k_f A_{c,0},$$

where  $A_{c,0} = 4\pi \left( \frac{3V_c}{4\pi} \right)^{2/3}$  is the surface area of the sphere of  $V_c$  volume.

In the general case, when both core- and shell-phases have a fractal shape, it is possible to use different shape factors for the external and internal interphase boundaries.

## Conclusion

For stratifying solutions, the UCDDT as well as the volume of the coexisting phases and the mutual solubility of the components depend on the system shape. A significant increase in the metastability region of the heterogeneous state provides for obtaining a continuous series of solid solutions at temperatures below the UCDDT and phases that do not occur in macroscopic systems. Such changes are possible with any change in geometric characteristics that change the area of interphase boundaries in small volume systems. The use of fractal geometry makes for significant extension of the application field of the model and the set of configurations under consideration.

Equally relevant is the case when a core-phase has fractal properties. This situation occurs when a new phase appears as a dendrite or suspension. The model with a fractal core-phase is relevant for studying the structure of crystalline deposit formed by drying up of colloidal solutions and biological fluids, in particular, to describe the "cafe-au-lait spots effect". The formation of such ring-shaped structures is typical for a wide range of systems that differ in physical nature and in the chemical composition of the dispersion medium, in the size and shape of particles in the dispersed phase [19-22]. The results are of interest in simulation of phase transformations in disperse systems, composite and polycrystalline materials.

\*

## Acknowledgment

*The research of Fedoseev V.B. is partially supported by the Russian Science Foundation, Grant No. 15-13-00137.*

## REFERENCES

- 1 Liang L.H., Liu D., Jiang Q. Size-dependent continuous binary solution phase diagram. *Nanotechnology*. 2003, Vol.14, No. 4, pp. 438 – 442.
- 2 Fedoseev V.B., Fedoseeva E.N. States of a supersaturated solution in limited-size systems. // *JETP Lett.* 2013. Vol. 97. No. 7, pp. 473-478.
- 3 Xue Y.-Q., Zhao M.-Z., Lai W.-P. Size-dependent phase transition temperatures of dispersed systems. *Phys. B Condens. Matter*. 2013, Vol. 408, pp. 134 – 139.
- 4 Bajaj S. et al. Phase stability in nanoscale material systems: extension from bulk phase diagrams. *Nanoscale*. 2015, Vol. 7, No. 21, pp. 9868 – 9877.
- 5 Fedoseev V.B., Fedoseeva E.N. Size effects during phase transformations in stratifying systems. // *Russ. J. Phys. Chem.* 2014. Vol. 88, No. 3, pp. 446 - 451.
- 6 Fedoseev V.B. Splitting of the phase diagram of a stratifying solid solution in micro- and nanosized systems. // *Phys. Solid State*. 2015. Vol. 57. No. 3, pp. 585-589.
- 7 Hourlier D., Perrot P. Au-Si and Au-Ge Phases Diagrams for Nanosystems. *Mater. Sci. Forum*. 2010, Vol. 653, pp. 77 – 85.
- 8 Tanaka T., Hara S. Thermodynamic evaluation of binary phase diagrams of small particle systems. *Zeitschrift fur Met.* 2001, Vol. 92, No. 11, pp. 467 – 472.
- 9 Magnin Y. et al. Size Dependent Phase Diagrams of Nickel-Carbon Nanoparticles. *Phys. Rev. Lett.* 2015, Vol. 115, No. 20, pp. 205502.

- 10 Fedoseev V.B., Shishulin A.V., Titaeva E.K., Fedoseeva E.N. On the possibility of the formation of a NaCl-KCl solid-solution crystal from an aqueous solution at normal temperature in small-volume systems. // *Phys. Solid State*. 2016. Vol. 58. No. 10, pp. 2020 - 2025.
- 11 Guisbiers G. et al. Size and Shape Effects on the Phase Diagrams of Nickel-Based Bimetallic Nanoalloys. *J. Phys. Chem. C*. 2017, Vol. 121, No.12, pp. 6930 – 6939.
- 12 Dahan Y., Makov G., Shneck R.Z. Nanometric size-dependent phase diagram of Bi-Sn. *Calphad*. 2016, Vol. 53, pp. 136 – 147.
- 13 Sutter E.A., Sutter P.W. Size-dependent phase diagram of nanoscale alloy drops used in vapor-liquid-solid growth of semiconductor nanowires. *ACS Nano*. 2010, Vol. 4, No. 8, pp. 4943-7.
- 14 Cholakova D. et al. Control of drop shape transformations in cooled emulsions. *Adv. Colloid Interface Sci*. 2016, Vol. 235, No. September, pp. 90 – 107.
- 15 Bykov M.A., Voronin G.F., Mukhamedzhanova N.M. *Direct and inverse problems of chemical thermodynamics*. Novosibirsk: Nauka, 1987, pp. 30 - 33.
- 16 Babichev A.P., Babushkina N.A., Bratkovsky A.M. et al. Physical quantities. *A reference guide*. Moscow: Energoatomizdat, 1991, 1232 p.
- 17 Fedoseev V.B. The use of fractal geometry for the thermodynamic description of three -dimensional elements of the crystal structure. *Letters on materials*. 2012, Vol. 2, pp. 78 - 83.
- 18 Fedoseev V.B. Thermodynamic analysis of the fractal dimension of crystal structure defects. *The nonlinear world*. 2009, Vol. 7, No.10, pp. 782 - 786.
- 19 Andreeva L.V., Novoselova A.S., Ivanov D.A. et al. Regularities of crystallization of dissolved substances from a microdroplet. *Technical Physics*. 2007, Vol.77, No. 2, pp. 22-30.
- 20 Yakhno T.A., Yakhno V.G. Fundamentals of the structural evolution of drying drops of biological fluids. *Technical Physics*. 2009. Vol. 79, No. 8, pp. 133-141.
- 21 Chikanova E.S., Fedoseev V.B., Golovanova O.A. Biofluids and fractals: a quantitative criterion for the self-organization of a drop. *Bulletin of Omsk State University*. 2015, No. 4, pp. 45-49.
- 22 Molchanov S.P., Roldugin V.I., Chernova-Kharaeva I.A. Three scenarios of evaporation of microliter droplets of dispersions and the structure of formed ring-shaped deposits. *Colloid Journal*. 2015, Vol. 77, No.6, pp. 764-774.